Volume 1 | Number 1 | Jan 2013 | Pages 1–100

ChemComm

Chemical Communications
www.rsc.org/chemcomm

ROYAL SOCIETY OF CHEMISTRY

This is an *Accepted Manuscript*, which has been through the Royal Society of Chemistry peer review process and has been accepted for publication.

Accepted Manuscripts are published online shortly after acceptance, before technical editing, formatting and proof reading. Using this free service, authors can make their results available to the community, in citable form, before we publish the edited article. We will replace this *Accepted Manuscript* with the edited and formatted *Advance Article* as soon as it is available.

You can find more information about *Accepted Manuscripts* in the **Information for Authors**.

Please note that technical editing may introduce minor changes to the text and/or graphics, which may alter content. The journal's standard **Terms & Conditions** and the **Ethical guidelines** still apply. In no event shall the Royal Society of Chemistry be held responsible for any errors or omissions in this *Accepted Manuscript* or any consequences arising from the use of any information it contains.

ChemComm

COMMUNICATION

A 9,9'-Spirobi[9H-fluorene]-Cored Perylenediimide Derivative and Its Application in Organic Solar Cells as Non-Fullerene Acceptor

Jinduo Yi[a,b], Yiling Wang[a,b], Qun Luo[a], Yi Lin[c], Hongwei Tan[d], Hongyu Wang[b], Chang-Qi Ma[a]*

A structurally non-planar molecule (SBF-PDI$_4$) with a 9,9'-spirobi[9H-fluorene] (SBF) core and four perylenediimide (PDI) at periphery was designed, synthesized and characterized. This compound shows a low-lying LUMO energy level of -4.11 eV, which is similar to that of PCBM, but with intensive light absorption ability over 450-550 nm. A high power conversion efficiency (PCE) of 5.34% was obtained for solution processed bulk heterojunction solar cell (BHJSC) using SBF-PDI$_4$ as the electron acceptor and a low-band gap polymer poly[[4,8-bis[5-(2-ethylhexyl)thiophene-2-yl]benzo[1,2-b:4,5-b']dithiophene-2,6-diyl][3-fluoro-2-[(2-ethylhexyl)carbonyl]thieno[3,4-b]thiophenedi-yl]] (PTB7-Th) as the electron donor. These results demonstrate that PDI derivatives with a three dimensional molecular structure could serve as high performance electron acceptor in BHJSCs.

Solution-processed polymer bulk-heterojunction organic solar cells (BHJ-OSCs) have received intensive attention because of their unique advantages such as low cost, light weight, ease of fabrication by large-scale, roll-to-roll printing techniques, and feasibility of flexible devices.[1-3] Very recently, power conversion efficiencies (PCEs) of 10-11% have been achieved for single-junction polymer/fullerene based solar cells.[4-7] Although fullerene derivatives with unique phase separation property and multidimensional charge transporting capabilities played a central role as electron acceptor in BHJ PSCs, drawbacks including weak absorption of visible light, poor chemical and electronic tunability, tedious purification and high production cost are also not ignorable. Moreover, despite the successes in laboratory scale devices, fullerenes are not an ideal material for production on an industrial scale. In contrast, non-fullerene acceptors in OSCs devices can avoid the drawbacks of fullerenes to some extent. Nowadays, solution-processed polymer/polymer[8, 9] and polymer/small molecule[10-12] BHJ-OSCs based on non-fullerene acceptors have shown PCEs up to 5-8%.[13, 14] However, non-fullerene acceptors are still lags behind fullerene derivatives, and new design routes for developing high performance non-fullerene acceptors are still highly needed.

Among the non-fullerene acceptors exploited so far for organic solar cells, perylenediimide (PDI) derivatives are the most frequently explored ones due to their excellent optical and electric properties, such as strong light absorption in the visible region between 400 nm to 650 nm, low-lying LUMO levels (about -4.0 eV), high electron mobilities (10^1-10^{-3} cm^2·V^{-1}·s^{-1}), simplicity in synthesis and purification processes, as well as chemically, thermally, and environmentally robust.[15] In the early stage, PDI derivatives for use in OSCs are typically with a planar molecular structure, and large crystalline domains (around 1 µm in size) are usually formed in the donor-acceptor blended film, which generally leads to poor photovoltaic performance.[16] To reduce the aggregation tendency of PDI-based small molecules, alkyl chains have been introduced on the bay or the "N" position of the PDI. However, not much improvement was achieved in such molecular modification method.[15] Very recently, a twisted PDI-dimer by linking two PDI units with various spacers, such as C-C single bond,[17] vinyl,[18] thiophene,[19] selenophene,[20] benzene,[19] biphenyl,[21] or spirofluorene[19, 22] have been developed. Such a twisted molecular structure effectively reduces the intermolecular interactions and thus hinders molecular aggregations. Performance of OSCs based on these materials was consequently improved.

Knowing that conjugated molecules with a three dimensional structure might form solid film with isotropic charge transport ability, development of new electron acceptor materials with 3D molecular structures has become an emerging topic. For example, Jenekhe and co-workers recent reported the development of non-fullerene small molecular acceptors with a 3D architecture.[23] Zhan et al. have reported a novel acceptor with triphenylamine as a core that has a quasi-3D nonplanar structure to reach a PCE of 3.32%.[24] Yan and Chen et al. also reported a series of 3D structure novel small molecular acceptors based on tetraphenylethylene,[21] tetraphenylmethane,[25] tetraphenylsilane,[25, 26] tetraphenylger-mane[25] core, enabling efficient polymer solar cells with a PCE of up to 5.53%.

[a.] Printable Electronics Research Center, Suzhou Institute of Nano-Tech and Nano-Bionics (SINANO), Chinese Academy of Sciences, 398 Ruo Shui Road, SEID SIP, Suzhou, 215123, P. R. China.
[b.] Department of chemistry, College of science, Shanghai University, 99 Shangda Road, BaoShan District 200444, Shanghai, P. R. China.
[c.] Department of Chemistry, Xi'an Jiaotong Liverpool University, 111 Ren Ai Road, SEID SIP, Suzhou, 215123, P. R. China.
[d.] College of Chemistry, Beijing Normal University, Beijing, 100875, PR China.
E-mail address: Chang-Qi Ma, cqma2011@sinano.ac.cn
†Electronic Supplementary Information (ESI) available: See DOI: 10.1039/x0xx00000x

It is known that 9,9'-spirobi[9H-fluorene] (SBF) is a well-developed spiro-molecule with an orthogonal molecular structure, where two planar fluorene unit are connected through an spiro-sp[3] carbon. This rigid and orthogonal core unit could serve as an excellent building block for constructing novel 3D molecules. In addition, a better solubility and less intensive intermolecular interaction of the final molecules would be expected for its nonplanar molecular structure.[27] However, only few PDI derivatives based on this well-known spiro-core were reported in the literatures.[19, 22] In this paper, we report the synthesis and characterization of a novel 3D PDI acceptor (**SBF-PDI$_4$**, Scheme 1) with a 9,9'-spirobi[9H-fluorene] core. A promising PCE of 5.34% was obtained by using a narrow-bandgap polymer material poly[[4,8-bis[5-(2-ethylhexyl)thiophene-2-yl]benzo[1,2-b:4,5-b'] dithiophene-2,6-diyl][3-fluoro-2-[(2-ethylhexyl)carbonyl]thieno [3,4-b]thiophe-nediyl]] (PTB7-Th) (Chart S1, ESI†) as donor. During the revision of this article, Cho et al. reported also the synthesis and use of spirobifluorene cored-PDI derivative as electron acceptor in organic solar cells.[28] These results suggest that structurally orthogonal PDI derivatives could serve as high performance electron acceptor in organic solar cells.

Scheme 1. Synthetic route to **SBF-PDI$_4$**.
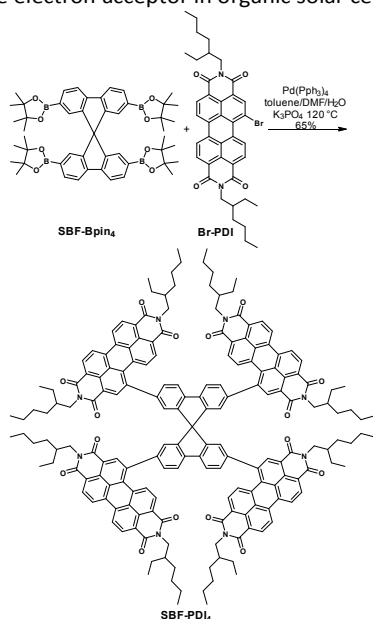
The synthetic route of **SBF-PDI$_4$** is outlined in Scheme 1. The target product **SBF-PDI$_4$** was synthesized in a middle yield of 65% by Suzuki coupling of Br-PDI with SBF-Bpin$_4$, which was synthesized by a palladium catalysed borylation.[29] This new compound was fully characterized with ^{1}H NMR, ^{13}C NMR, MALDI-TOF-MS spectroscopy (ESI†). **SBF-PDI$_4$** showed a higher solubility in chloroform, dichloromethane, dichlorobenzene and chlorobenzene than the corresponding linear analogue **PDI-F-PDI** (Scheme S1, ESI†), which was attributed to the non-planar molecular structure of **SBF-PDI$_4$**.

The geometries of SBF-PDI4 and PDI-F-PDI were optimized using the Gaussian09 program with B3LYP/6-31G(d,p) approach. As shown in Fig. S1 (ESI†), in PDI-F-PDI, the dihedral between PDI plane and the fluorene plane is 122.5 degree, while in SBF-PDI$_4$, due to the steric repulsion between PDI rings, the PDI rings align almost vertical (83.7 degree) to the

adjacent fluorene plane (Fig. S1, left; ESI†). The frontier molecular orbital (FMO) diagrams of SBF-PDI4 and PDI-F-PDI are shown in Fig. S2 and Fig. S3 (ESI†). According to the calculated results, the FMOs of SBF-PDI$_4$ and PDI-F-PDI consist mainly of the molecular orbitals from the PDI rings. Since there are four PDI rings in SBF-PDI$_4$ and only two PDI rings in PDI-F-PDI, the HOMOs and LUMOs of SBF-PDI$_4$ are quasi quadra-degenerated, while those of PDI-F-PDI are quasi double-degenerated.

UV-vis absorption spectra of **SBF-PDI$_4$** in chloroform solution and in thin film are presented in Fig. 1(a), and their corresponding data are summarized in Table 1. The absorption spectra of **SBF-PDI$_4$** in solution exhibit a strong absorption band over 450-550 nm with a peak absorption at 535 nm. The molecular mole extinction coefficient was determined to be 93,300 mol^{-1}·L·cm^{-1}. The absorption maximum of **SBF-PDI$_4$** in thin solid film shows a 10 nm red-shift when compared to that in solution (Fig. 1(a) and table 1). A broader absorption with a similar profile was found for the solid film absorption, suggesting weak intermolecular interactions in solid film. The optical band gaps calculated from the absorption onset wavelength (λ_{onset}^{film}) was 2.03 eV for **SBF-PDI$_4$** which is similar to other PDI based acceptor materials.[21, 26]

Electrochemical characterization of **SBF-PDI$_4$** was carried out by cyclic voltammetry (CV) in dichloromethane solution. The cyclic voltammogram and differential pulse voltammogram (DPV) are shown in Fig. 1(b), and the relevant data are compiled in Table 1. As can be seen from Fig. 1(b), **SBF-PDI$_4$** exhibits quasi-reversible redox processed both at positive and negative potential range. The measured oxidation potentials were ascribed to the oxidation processes of the spirobifluorene core,[30] whereas the reduction potentials were related to the reduction of the PDI units.[24, 30] By DPV measurement the two oxidation potentials (vs. Fc$^+$/Fc) were determined to be 1.21 and 1.39 V, respectively. Three reduction processes (E_{red}^0 = -1.02, -1.16 and -1.29 V) were determined from the DPV measurement, which is different to that of the PDI monomers,[31] suggesting possible intramolecular interaction between the four peripheral PDI units. The HOMO/LUMO energy levels of **SBF-PDI$_4$** were calculated according to the following equations: E_{LUMO} = -(E_{red}^{onset} + 5.10) [eV] and E_{HOMO} = - (E_{ox}^{onset} + 5.10) [eV], where, the standard energy level for Fc/Fc$^+$ was taken as -5.10 eV.[32] The HOMO/LUMO energy level data are also listed in **Table 2**. As can be seen from this Table, the LUMO energy level of **SBF-PDI$_4$** (-4.11 eV) is slightly lower than that of [6,6]-phenyl-C$_{61}$-butyric acid methyl ester (PC$_{61}$BM, -4.01 eV), indicating **SBF-PDI$_4$** could serve as an electron acceptor in organic solar cells.

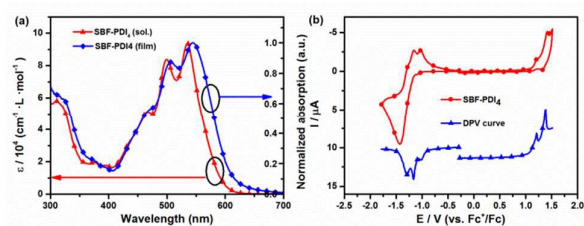Organic solar cells with an inverted structure of ITO/ZnO (20

Fig. 1 (a) UV-vis absorption spectra of **SBF-PDI$_4$** in chloroform solution at 9×10^{-6} mol·L^{-1} and in thin film. (b) Cyclic voltammetry (CV) of **SBF-PDI$_4$** (in dichloromethane solution, at 1.0×10^{-3} mol·L^{-1}, with 0.1 mol·L^{-1} Bu$_4$NPF$_6$ as the supporting electrolyte)

COMMUNICATION

Table 1 Photophysical data of **SBF-PDI₄** and PC₆₁BM.

Compound	$\lambda_{max}^{sol.}$ [nm]a	$\varepsilon_{max}^{sol.}$ [mol⁻¹·L·cm⁻¹]b	$\lambda_{onset}^{sol.}$ [nm]a	λ_{max}^{film} [nm]c	$\lambda_{onset}^{film.}$ [nm]c	E_g^{opt}(film) [eV]d	E_{red1}^0 [V]e	E_{red2}^0 [V]e	E_{red3}^0 [V]e	E_{ox1}^0 [V]e	E_{ox2}^0 [V]e	E_{HOMO} [eV]f	E_{LUMO} [eV]f	E_g^{cv} [eV]g	Ref.
SBF-PDI₄	535	93,300	593	545	611	2.03	-1.02	-1.16	-1.29	1.21	1.39	-6.24	-4.11	2.13	This work
PC₆₁BM	331	49,000	--	--	--	--	-1.16	-1.42	--	1.19	--	-5.95	-4.01	1.94	[33]

a In CHCl₃ solution (9.0 × 10⁻⁶ mol·L⁻¹); b Extinction coefficient in solution was obtained by linear fitting absorbance vs. concentration (ESI†); c Film was prepared by spin-coating CHCl₃ solution onto the quartz; d Optical band gap in solid film, E_g^{opt} (eV) = 1240/ λ_{onset}^{film} [nm]. e Determined from DPV measurements. f Calculated from the cyclic voltammograms, $E_{LUMO} = -[E_{onset}^{red} + 5.1]$ (eV), $E_{HOMO} = -[E_{ox}^{red} + 5.1]$ (eV) where the vacuum energy level of Fc⁺/Fc was set as -5.1 eV; g Electrochemical band gap calculated from the E_g^{cv}[eV] = E_{LOMO}-E_{HUMO} (eV).

nm)/active layer (~ 100 nm)/MoO₃ (20 nm)/Al (100 nm) were fabricated with the blended films of PTB7-Th:**SBF-PDI₄** as the photoactive layer. The ratio of donor to acceptor (D/A) was optimized using chloroform as the processing solvent, and results show that the best D/A ratio is 1:1 (*w/w*) (see **Table S1**, ESI†). Then, the influence of additive of *1*-chloronaphthalene (CN) on the performance of PTB7-Th:**SBF-PDI₄** cell was carefully examined. The detailed photovoltaic parameters of the OSC devices with different D/A ratios and additive amounts are listed in **Table 2** and **Table S1** (ESI†). Without using any co-solvents, all the PTB7-Th:**SBF-PDI₄** based devices worked and gave well-reproducible performances. The best PCE was 3.66% with an open voltage V_{OC} = 0.86 V, short current density J_{SC} = 8.82 mA·cm⁻², and fill factor FF = 0.48. Surprisingly, the V_{OC} of 0.86 V was found to be higher than the value of PTB7-Th:PC₆₁BM (V_{oc} = 0.79 V) based devices, although the LUMO of **SBF-PDI₄** is lower than that of PC₆₁BM. There are many factors that influence the V_{OC} of solar cells,[34] it is rather difficult to explain the exact reason for the high V_{OC} of SBF-PDI₄ based device. However, since these two compounds have totally different molecular structures, the higher V_{OC} of PTB7-Th:SBF-PDI₄ based device could be due to the 3D-

molecular structure of SBF-PDI₄ which leads to a higher Fermi energy level (E_F) of SBF-PDI₄ in solid state. On the basis of the optimal D/A ratio, the effect of additive (CN) content on the performance of the PTB7-Th:**SBF-PDI₄** based devices were investigated. As a result, the average PCE increased continuously, which was mainly attributed to the higher J_{sc} than without any additive when CN was added (see Table S1, ESI†). The J_{SC} increased dramatically from 8.82 mA·cm⁻² to 13.08 mA·cm⁻², while the V_{OC} has little decrease from 0.86 V to 0.85 V and the FF are essentially constant. The highest efficiency devices were fabricated with 1.0% (*v/v*) CN as additive, showing a best PCE of 5.34% and an average PCE of 5.26%. As comparison, the linear molecular **PDI-F-PDI** based device showed a best PCE of 3.97% (ESI†), which is much lower than that of **SBF-PDI₄** based devices. Fig. 2(b) shows the external quantum efficiency (EQE) spectra of the optimal cells. The EQE responses cover a wavelength range from 300 to 800 nm, and these responses correspond well to the UV-vis absorption spectrum of the corresponding 1:1 (*w/w*) blend films (Fig. 2(b) and Fig. S4, ESI†), unequivocally confirmed that absorption of **SBF-PDI₄** contribute to the J_{SC} in these devices.

It is well known that good electron transport properties are another key factor for high performance acceptor materials. The electron mobility of **SBF-PDI₄** was measured by the space charge limited current (SCLC) method with a device structure of ITO/ZnO/PTB7-Th:**SBF-PDI₄**/LiF/Al. Fig. S6 (ESI†) depicts the double logarithmic *J-V* curves of **SBF-PDI₄** based electron only devices with different layer thickness. From these curves, we can know that all these log(*J*)-log(*V*) cures showed two linear regime with different slopes. At low voltage ranges (0-0.3V), the slope was determined to be 1.09 suggesting an ohmic behavior at low bias. At the second regime with a slope of 2.03 was found at higher bias (0.5V-8V), suggesting a possibility of space-charge limited current (SCLC) behaviour at such a voltage range. The fact that current was inversely proportional to the cube of thickness of the active layer (Fig. S6(b), ESI†) further confirmed the space-charge limited current. The
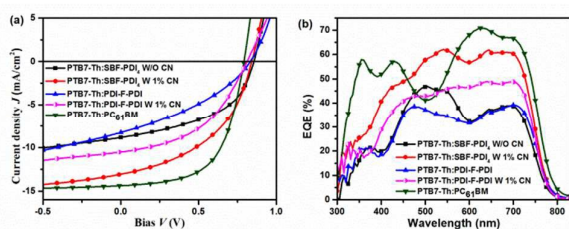

Fig. 2 (a) J–V curves and (b) EQE spectra of PTB7-Th:**SBF-PDI₄** (*w/w*; 1:1) with/without CN as additive, PTB7-Th:PDI-F-PDI (*w/w*; 1:1) and PTB7-Th:PC₆₁BM based devices.

Table 2. Photovoltaic properties of solar cells based on devices using PTB7-Th as donor, SBF-PDI₄, SF-PDI₂, PDI-F-PDI and PC₆₁BM as electron acceptors.

Acceptor	V_{OC} (V)	J_{SC} (mA·cm⁻²)a	FF	PCE (%)	Aver. PCEb (± std. dev.)(%)
SBF-PDI₄	0.86	8.82	0.48	3.66	3.45 (±0.112)c
	0.85	13.08	0.48	5.34	5.26 (±0.102)d
SF-PDI₂	1.01	7.60	0.39	3.00	2.9 (±0.102)f
PDI-F-PDI	0.84	8.27	0.36	2.49	2.44 (±0.045)c
	0.82	10.52	0.46	3.97	3.85 (±0.108)d
PC₆₁BM	0.80	14.40	0.61	7.03	6.96 (±0.082)e

a calculated by convoluting the spectral response with the AM 1.5G spectrum (100 mW·cm⁻²); bAverage values from over 8 pieces of devices. Tested under illumination of AM 1.5G 100 mW·cm⁻²; c without additive; d with 1% CN; e with 3% 1,8-diiodooctane (DIO); f ref.[22].
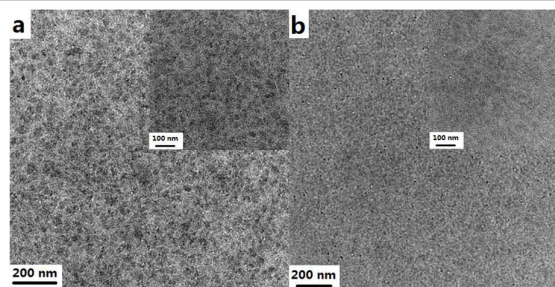

Fig. 3 TEM images of PTB7-Th:**SBF-PDI₄** blend films (a) without CN, (b) with 1% CN.

electron mobility was then calculated to be 1.33×10^{-4} $cm^2 \cdot V^{-1} \cdot s^{-1}$ according to the Mott–Gurney law, which is close to those of PDI derivatives reported in the literatures.[21, 24, 26]

Transmission electron microscopy (TEM) was also used to investigate the influence of the CN additive on the morphology of the active layer. Fig. 3 displays the TEM images of PTB7-Th:**SBF-PDI₄** (1:1) blend films without/with 1% CN additive. As shown in this figure, thin film blends processed without CN formed large phase separated domains (center-to-center spacing of 30-40 nm). These dimensions are much larger than typical organic exciton diffusion lengths of 10 nm[35] and thereby severely limit device performance. The low J_{SC} for the devices fabricated without additive are attributed to this partially over-sized phase separation. By using 1% CN as the additive, more homogeneous morphology with a uniform nano-structure (about 10 nm) appears, which is favourable for the exciton dissociation, leading to increased J_{SC} values.

In summary, a 3D structured molecule (**SBF-PDI₄**) based on perylenediimide (**PDI**) and 9,9'-spirobi[9H-fluorene] (**SBF**) core was designed, synthesized and characterized. The synthesized **SBF-PDI₄** shows good solubility in common organic solvents. The photophysical and electrochemical properties of **SBF-PDI₄** were also measured. The electron mobility was calculated to be 1.33×10^{-4} $cm^2 \cdot V^{-1} \cdot s^{-1}$ using electron only devices by SCLC method. When blended with the conjugated polymer donor of PTB7-Th in solution-processed BHJ-OSCs, a PCE of 5.34% was obtained, which was much higher than that of device using linear compound **PDI-F-PDI**. These results demonstrate that fine-tuning of PDI-based materials with a 3D configuration maybe is a promising way in developing high performance non-fullerene electron acceptors for BHJSCs.

Notes and references

1. F. C. Krebs, M. Jørgensen, K. Norrman, O. Hagemann, J. Alstrup, T. D. Nielsen, J. Fyenbo, K. Larsen and J. Kristensen, *Sol. Energy Mater. Sol. Cells*, 2009, **93**, 422-441.
2. T. D. Nielsen, C. Cruickshank, S. Foged, J. Thorsen and F. C. Krebs, *Sol. Energy Mater. Sol. Cells*, 2010, **94**, 1553-1571.
3. L. Lu, T. Zheng, Q. Wu, A. M. Schneider, D. Zhao and L. Yu, *Chem. Rev.*, 2015, DOI: 10.1021/acs.chemrev.5b00098.
4. L. K. Jagadamma, M. Al-Senani, A. El-Labban, I. Gereige, G. O. N. Ndjawa, J. C. D. Faria, T. Kim, K. Zhao, F. Cruciani, D. H. Anjum, M. A. McLachlan, P. M. Beaujuge and A. Amassian, *Adv. Energy. Mater.*, 2015, **5**, DOI: 10.1002/aenm.201500204.
5. S. Zhang, L. Ye, W. Zhao, B. Yang, Q. Wang and J. Hou, *Sci. China Chem.*, 2015, **58**, 248-256.
6. V. Vohra, K. Kawashima, T. Kakara, T. Koganezawa, I. Osaka, K. Takimiya and H. Murata, *Nat. Photon.*, 2015, **9**, 403-408.
7. Y. Liu, J. Zhao, Z. Li, C. Mu, W. Ma, H. Hu, K. Jiang, H. Lin, H. Ade and H. Yan, *Nat. Commun.*, 2014, **5**, 5293.
8. Y. J. Hwang, B. A. Courtright, A. S. Ferreira, S. H. Tolbert and S. A. Jenekhe, *Adv. Mater.*, 2015, **27**, 4578-4584.
9. J. W. Jung, J. W. Jo, C. C. Chueh, F. Liu, W. H. Jo, T. P. Russell and A. K. Jen, *Adv. Mater.*, 2015, **27**, 3310-3317.
10. Y. J. Hwang, H. Li, B. A. Courtright, S. Subramaniyan and S. A. Jenekhe, *Adv. Mater.*, 2015, DOI: 10.1002/adma.201503801.
11. K. Cnops, B. P. Rand, D. Cheyns, B. Verreet, M. A. Empl and P. Heremans, *Nat. Commun.*, 2014, **5**, 3406.
12. H. Lin, S. Chen, Z. Li, J. Y. Lai, G. Yang, T. McAfee, K. Jiang, Y. Li, Y. Liu, H. Hu, J. Zhao, W. Ma, H. Ade and H. Yan, *Adv. Mater.*, 2015, DOI: 10.1002/adma.201502775.
13. C. B. Nielsen, S. Holliday, H. Y. Chen, S. J. Cryer and I. McCulloch, *Acc. Chem. Res.*, 2015, DOI: 10.1021/acs.accounts.5b00199.
14. Y. Z. Lin and X. W. Zhan, *Adv. Energy. Mater.*, 2015, **5**, DOI: 10.1002/aenm.201501063.
15. Y. Lin and X. Zhan, *Mater. Horizons*, 2014, **1**, 470-488.
16. J. J. Dittmer, E. A. Marseglia and R. H. Friend, *Adv. Mater.*, 2000, **12**, 1270-1274.
17. Y. Zang, C. Z. Li, C. C. Chueh, S. T. Williams, W. Jiang, Z. H. Wang, J. S. Yu and A. K. Jen, *Adv. Mater.*, 2014, **26**, 5708-5714.
18. Y. Zhong, M. T. Trinh, R. Chen, W. Wang, P. P. Khlyabich, B. Kumar, Q. Xu, C. Y. Nam, M. Y. Sfeir, C. Black, M. L. Steigerwald, Y. L. Loo, S. Xiao, F. Ng, X. Y. Zhu and C. Nuckolls, *J. Am. Chem. Soc.*, 2014, **136**, 15215-15221.
19. Q. Yan, Y. Zhou, Y.-Q. Zheng, J. Pei and D. Zhao, *Chem. Sci.*, 2013, **4**, 4389-4394.
20. X. Zhang, J. Yao and C. Zhan, *Chem. Commun.*, 2015, **51**, 1058-1061.
21. Y. Liu, C. Mu, K. Jiang, J. Zhao, Y. Li, L. Zhang, Z. Li, J. Y. Lai, H. Hu, T. Ma, R. Hu, D. Yu, X. Huang, B. Z. Tang and H. Yan, *Adv. Mater.*, 2015, **27**, 1015-1020.
22. J. Zhao, Y. Li, H. Lin, Y. Liu, K. Jiang, C. Mu, T. Ma, J. Y. Lin Lai, H. Hu, D. Yu and H. Yan, *Energy Environ. Sci.*, 2015, **8**, 520-525.
23. H. Li, T. Earmme, G. Ren, A. Saeki, S. Yoshikawa, N. M. Murari, S. Subramaniyan, M. J. Crane, S. Seki and S. A. Jenekhe, *J. Am. Chem. Soc.*, 2014, **136**, 14589-14597.
24. Y. Lin, Y. Wang, J. Wang, J. Hou, Y. Li, D. Zhu and X. Zhan, *Adv. Mater.*, 2014, **26**, 5137-5142.
25. Y. H. Liu, J. Y. L. Lai, S. S. Chen, Y. K. Li, K. Jiang, J. B. Zhao, Z. K. Li, H. W. Hu, T. X. Ma, H. R. Lin, J. Liu, J. Zhang, F. Huang, D. M. Yu and H. Yan, *J. Mater. Chem. A*, 2015, **3**, 13632-13636.
26. S.-Y. Liu, C.-H. Wu, C.-Z. Li, S.-Q. Liu, K.-H. Wei, H.-Z. Chen and A. K. Y. Jen, *Adv. Sci.*, 2015, **2**, 1500014-1500020.
27. T. P. Saragi, T. Spehr, A. Siebert, T. Fuhrmann-Lieker and J. Salbeck, *Chem. Rev.*, 2007, **107**, 1011-1065.
28. J. Lee, R. Singh, D. H. Sin, H. G. Kim, K. C. Song and K. Cho, *Adv. Mater.*, 2015, DOI: 10.1002/adma.201504010.
29. S. Ma, Y. Fu, D. Ni, J. Mao, Z. Xie and G. Tu, *Chem. Commun.*, 2012, **48**, 11847-11849.
30. C. Y. Chan, Y. C. Wong, H. L. Wong, M. Y. Chan and V. W. W. Yam, *J. Mater. Chem. C*, 2014, **2**, 7656-7665.
31. J. Yi, Y. Ma, J. Dou, Y. Lin, Y. Wang, C.-Q. Ma and H. Wang, *Dyes and Pigments* in press.
32. C. M. Cardona, W. Li, A. E. Kaifer, D. Stockdale and G. C. Bazan, *Adv. Mater.*, 2011, **23**, 2367-2371.
33. J. Wu, Y. Ma, N. Wu, Y. Lin, J. Lin, L. Wang and C. Q. Ma, *Org. Electron.*, 2015, **23**, 28-38.
34. N. K. Elumalai and A. Uddin, *Energy Environ. Sci.*, 2015, DOI: 10.1039/c5ee02871j.
35. P. E. Shaw, A. Ruseckas and I. D. W. Samuel, *Adv. Mater.*, 2008, **20**, 3516-3520.